

Analysis of Ca^{2+} uptake into the smooth endoplasmic reticulum of permeabilised sternal epithelial cells during the moulting cycle of the terrestrial isopod *Porcellio scaber*

Monica Hagedorn and Andreas Ziegler*

Zentrale Einrichtung Elektronenmikroskopie, Universität Ulm, 89069 Ulm, Germany

*Author for correspondence (e-mail: andreas.ziegler@medizin.uni-ulm.de)

Accepted 18 April 2002

Summary

In terrestrial isopods, large amounts of Ca^{2+} are transported across anterior sternal epithelial cells during moult-related deposition and resorption of CaCO_3 deposits. Because of its toxicity and function as a second messenger, resting cytosolic Ca^{2+} levels must be maintained below critical concentrations during epithelial Ca^{2+} transport, raising the possibility that organelles play a role during Ca^{2+} transit. We therefore studied the uptake of Ca^{2+} into Ca^{2+} -sequestering organelles by monitoring the formation of birefringent calcium oxalate crystals in permeabilised anterior and posterior sternal epithelium cells of *Porcellio scaber* during Ca^{2+} -transporting and non-transporting stages of the moulting cycle using polarised-light microscopy. The results indicate ATP-dependent uptake of Ca^{2+} into organelles. Half-maximal crystal growth at a Ca^{2+} activity, a_{Ca} , of $0.4 \mu\text{mol l}^{-1}$ and blockade by cyclopiazonic acid suggest

Ca^{2+} uptake into the smooth endoplasmic reticulum by the smooth endoplasmic reticulum Ca^{2+} -ATPase. Analytical electron microscopical techniques support this interpretation by revealing the accumulation of Ca^{2+} -containing crystals in smooth membranous intracellular compartments. A comparison of different moulting stages demonstrated a virtual lack of crystal formation in the early premoult stage and a significant fivefold increase between mid premoult and the Ca^{2+} -transporting stages of late premoult and intramoult. These results suggest a contribution of the smooth endoplasmic reticulum as a transient Ca^{2+} store during intracellular Ca^{2+} transit.

Key words: calcium oxalate, Crustacea, epithelial Ca^{2+} transport, biomineralisation, smooth endoplasmic reticulum Ca^{2+} -ATPase, SERCA, sequestration, Ca^{2+} -ATPase, isopod, *Porcellio scaber*.

Introduction

The rapid bidirectional Ca^{2+} dynamics and high flux rates of Ca^{2+} during the moulting cycle (Neufeld and Cameron, 1993) make crustacean epithelia excellent model systems for the analysis of epithelial Ca^{2+} transport (Wheatly, 1997). The crustacean exoskeleton is mineralised mainly by CaCO_3 (Greenaway, 1985) and, in order to grow, crustaceans have to moult their cuticle periodically. The terrestrial isopod *Porcellio scaber* moults every 6 weeks and develops large sternal reservoirs containing amorphous, possibly hydrated, CaCO_3 (Drobne and Štrus, 1996; Ziegler, 1994) before every moult. The deposition and resorption of these reservoirs are linked to the unique biphasic moulting cycle of isopods in which first the posterior and then the anterior cuticle are shed. During premoult, calcium is resorbed from the posterior cuticle into the haemolymph and transported across the anterior sternal epithelium (ASE) to form CaCO_3 deposits between the epithelium of the integument and the old cuticle (Messner, 1965; Steel, 1993). Between the posterior and anterior half-body moults (intramoult), these CaCO_3 deposits are resorbed and used to mineralise the new posterior cuticle. Ultrastructural

studies have shown that the ASE differentiates for epithelial ion transport during the formation and resorption of these CaCO_3 deposits (Glötzner and Ziegler, 2000; Ziegler, 1996).

Ca^{2+} transport is generally either paracellular, between the epithelial cells, or transcellular. Transcellular Ca^{2+} transport can be divided into three phases: the passive influx of Ca^{2+} at one side of the epithelial cell, Ca^{2+} transport from one side of the cell to the other, and the energy-consuming extrusion of Ca^{2+} . In crustaceans, entry probably occurs through Ca^{2+} channels or by a $\text{Ca}^{2+}/\text{H}^+$ exchanger (Ahearn and Franco, 1990; Ahearn and Zhuang, 1996). Active extrusion of Ca^{2+} probably involves a Ca^{2+} -ATPase (Flik et al., 1994; Greenaway et al., 1995; Roer, 1980) or a $\text{Na}^+/\text{Ca}^{2+}$ exchanger (Ahearn and Franco, 1993). In the ASE of *P. scaber*, electron-probe microanalysis (Ziegler, 2002), expression analysis of the plasma membrane Ca^{2+} -ATPase and the $\text{Na}^+/\text{Ca}^{2+}$ exchanger (Ziegler et al., 2001) and the abundance of Na^+/K^+ -ATPase in the basolateral membrane (Ziegler, 1997) suggest that the transcellular pathway dominates.

How Ca^{2+} is transported within the epithelial cells is still

unknown. Because of the multiple physiological functions of Ca^{2+} , the mean free cytosolic Ca^{2+} concentration in cells is maintained at approximately $0.1 \mu\text{mol l}^{-1}$. Transient rises in Ca^{2+} concentration are tolerated, but high sustained Ca^{2+} concentrations in the cytoplasm are toxic and can lead to cell death (Berridge, 1993). A cytosolic route with Ca^{2+} bound to proteins (Feher et al., 1989) and an organellar route (Nemere, 1992; Simkiss, 1996) have therefore been proposed for Ca^{2+} transit. Simkiss (1996) proposed a model in which the smooth endoplasmic reticulum (SER) could function as a transient Ca^{2+} store, leading only to micromolar gradients in the cytoplasm. Electron-probe microanalysis on sternal epithelial cells of *P. scaber* showed a significant increase in the total (free plus bound) cytoplasmic Ca^{2+} concentration during the Ca^{2+} -transporting stages (Ziegler, 2002). It is of particular interest that this increase is due to an increase in the number of areas with Ca^{2+} concentrations of up to $50 \text{ mmol l}^{-1} \text{ kg}^{-1}$ dry mass because this is similar to the concentrations measured in the SER of bee photoreceptors (Baumann et al., 1991) and vertebrate skeletal muscle (Somlyo et al., 1981).

In an attempt to test the hypothesis that the SER contributes to epithelial Ca^{2+} transport, we investigated the smooth endoplasmic reticulum Ca^{2+} -ATPase (SERCA)-dependent uptake of Ca^{2+} during four different moulting stages in *P. scaber* employing an *in situ* calcium oxalate assay (Walz and Baumann, 1989). The results indicate an increase in SERCA-dependent Ca^{2+} uptake into the SER between the non-transporting and the Ca^{2+} -transporting moulting stages.

Materials and methods

Animal preparation

Porcellio scaber Latreille were maintained in plastic containers filled with soil and bark and fed on pieces of fresh potatoes and carrots. Adult non-breeding animals (body length 8.5–12 mm) at four different stages of the moulting cycle (early premoult, mid premoult, late premoult and intramoult) were used for the experiments. The animals in early and mid premoult were used 6 days and 2 weeks after the moult of the anterior part of the body, respectively. Well-developed sternal CaCO_3 deposits defined the late premoult stage. For intramoult (the period between posterior and anterior moult) animals, specimens with partly degraded CaCO_3 deposits were selected.

Animals were dissected in nominally Ca^{2+} -free (no calcium added) physiological saline containing 248 mmol l^{-1} NaCl, 8 mmol l^{-1} KCl, 10 mmol l^{-1} MgCl_2 , 5 mmol l^{-1} glucose and 10 mmol l^{-1} Tris, pH 7.4. Anterior and posterior sternal epithelia were dissected, and fatty tissue was carefully removed if necessary. Epithelia of animals in late premoult or intramoult already carried the first layers of unmineralised cuticle. Clean sternal epithelial cell layers were transferred onto nickel grids (200 mesh, thin bar, Plano Corporation) with the apical side facing away from the grid. The specimen and grid were then mounted in a perfusion chamber with the apical side facing up and with ready access of the solution to the basal side of the epithelium. A coverslip was placed on top of the

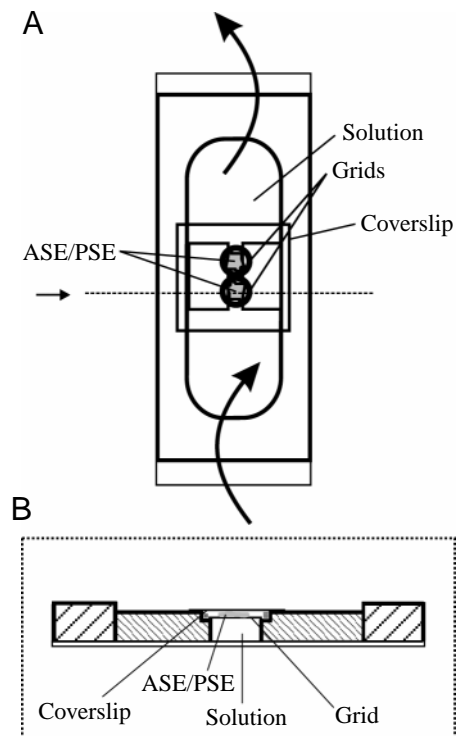


Fig. 1. (A) Schematic diagram of the perfusion chamber with anterior (ASE) and posterior (PSE) sternal epithelia mounted on grids. Solutions can be exchanged at the side of the chamber without disturbing the specimen (large arrows). (B) Side view of the perfusion chamber at the level indicated in A by the small arrow and a dotted line.

perfusion chamber leaving only a narrow gap above the mounted specimen (Fig. 1A,B). The chamber was then placed on the stage of a light microscope (Zeiss, Axiophot) equipped with polarisation filters. Whenever possible, anterior and posterior sternal epithelia were analysed simultaneously.

Calcium oxalate assay

The principle of the calcium oxalate assay for measurement of relative Ca^{2+} uptake rates into the Ca^{2+} -sequestering SER was described by Walz and Baumann (1989). In permeabilised cells, oxalate moves from a loading medium into the SER by an unknown mechanism. In the presence of ATP, the SERCA pumps Ca^{2+} into the lumen of the SER. When the oxalate and Ca^{2+} concentrations exceed the solubility product, birefringent calcium oxalate precipitates form within the SER lumen, and crystal growth can be monitored in a polarisation microscope as long as Ca^{2+} is transported into the lumen of the endoplasmic reticulum. After a calcium oxalate loading experiment, the birefringent calcium oxalate crystals appear bright against a dark background (Fig. 2).

For calcium oxalate loading experiments, the sternal epithelial cells were first permeabilised with $20 \mu\text{g ml}^{-1}$ saponin in 2 mmol l^{-1} K_2EGTA , 125 mmol l^{-1} KCl, 5 mmol l^{-1} MgCl_2 , 5 mmol l^{-1} Na_2ATP , 20 mmol l^{-1} Hepes, pH 7.0 (adjusted with KOH), for 20 min. After permeabilisation, the

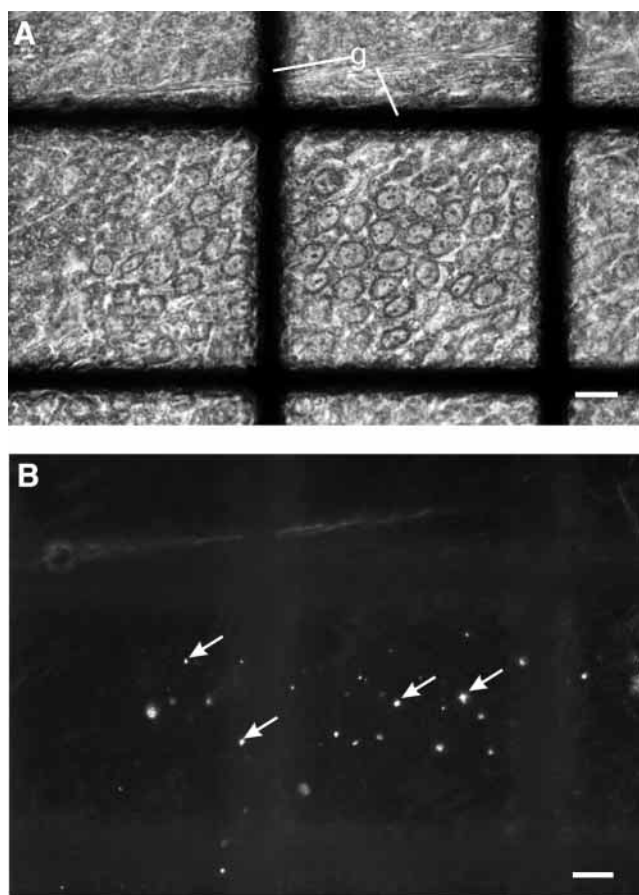


Fig. 2. Light micrographs, (A) phase-contrast and (B) polarisation microscopy image, of the anterior sternal epithelium of *Porcellio scaber* after a calcium oxalate loading experiment. The birefringent calcium oxalate crystals appear as bright signals (arrows). Scale bar, 20 μm . g, grid bar.

tissue was incubated under constant stirring in standard loading medium containing 1 mmol l^{-1} K_2EGTA , 125 mmol l^{-1} KCl , 5 mmol l^{-1} MgCl_2 , 5 mmol l^{-1} Na_2ATP , 25 mmol l^{-1} potassium oxalate, 4 mmol l^{-1} CaEGTA , 2.5 $\mu\text{g ml}^{-1}$ oligomycin, 5 $\mu\text{mol l}^{-1}$ carbonyl cyanide *m*-chlorophenylhydrazone (CCCP) and 20 mmol l^{-1} HEPES, pH 7.0 (adjusted with KOH). Oligomycin and CCCP were added to the loading medium to prevent calcium oxalate forming in the mitochondria. The Ca^{2+} activity (a_{Ca}) of the loading medium (0.68 $\mu\text{mol l}^{-1}$) was measured using Ca^{2+} -sensitive mini-electrodes (ETH129) prepared as described previously (Ziegler and Scholz, 1997) and calibrated using the solutions of Tsien and Rink (1980).

To measure the Ca^{2+} -dependency of calcium oxalate formation, we varied the a_{Ca} of the loading medium between 0.15 and 2.05 $\mu\text{mol l}^{-1}$ by changing the ratio of CaEGTA to K_2EGTA , keeping the total EGTA concentration constant at 5 mmol l^{-1} . ATP-dependency was demonstrated by omitting Na_2ATP from the loading medium. The effects of cyclopiazonic acid (CPA) (1 $\mu\text{mol l}^{-1}$), ryanodine (10 $\mu\text{mol l}^{-1}$ and 0.5 mmol l^{-1}) and caffeine (25 and 50 mmol l^{-1}) were investigated by adding the reagents to the loading medium at

various values of a_{Ca} . For experiments with inositol trisphosphate (InsP_3) (3 and 5 $\mu\text{mol l}^{-1}$), we reduced the MgCl_2 concentration of the loading medium to 2 mmol l^{-1} and repeated the experiments at various values of a_{Ca} .

All chemicals were purchased from Merck Corporation except Na_2ATP , saponin, CPA, CCCP and oligomycin, which were obtained from Sigma Corporation, and EGTA, which was obtained from Fluka Chemika Corporation.

A CCD camera (Visitron, Spot) was used to take sequences of grey-scale images with a 20 \times 0.50 objective (Zeiss) at 1 or 2 min intervals. We used TINA software (Raytest) for the digital analysis of transmitted light through the polariser and analyser (aligned in the crossed position). Mean grey-scale values in areas of $1.25 \times 10^3 \mu\text{m}^2$ were quantified for each image and are presented as the intensity change from that of the first image (Δ intensity units). Linear regression was used to calculate the relative amount of calcium oxalate formed from each series of images. Rates are given as intensity units min^{-1} , and values are presented as means \pm S.E.M. One-way analysis of variance (ANOVA) followed by the Tukey–Kramer multiple-comparison test was used for statistical analysis. Calculations were performed using GraphPad Prism 3.0 software.

Electron energy-loss spectroscopy and electron energy-loss imaging

Sternal epithelia were prepared, permeabilised and incubated in loading medium as described above. After loading the epithelial cells with calcium oxalate for 50 min, single sternites were high-pressure frozen at $2.3 \times 10^8 \text{ N m}^{-2}$ (Leica, EMHPF) and freeze-substituted in acetone containing 1% H_2O and 1% OsO_4 (P. Walther and A. Ziegler, unpublished data). Freeze-substitution was performed over a 22 h period using a custom-built computer-controlled device with the temperature rising exponentially from -90 to 0°C . After washing the specimens with pure acetone at room temperature (22°C), the samples were embedded in Epon resin. Ultrathin sections (20 nm) were cut on a Leica Ultracut microtome with the sections floating on glycerol to prevent loss of water-soluble calcium oxalate precipitates. The sections were viewed unstained in an energy-filtering transmission electron microscope (Zeiss CEM 902) at 80 kV using a 30 μm diameter objective aperture. Electron energy-loss imaging (ESI) micrographs were taken below and above the specific element energy loss edge, $L_{2,3}$ (346 eV) of calcium, at $\Delta E = 340 \pm 5 \text{ eV}$ and $\Delta E = 360 \pm 5 \text{ eV}$, where E is the energy of the electrons. Electron energy-loss (EEL) spectra were recorded in serial mode with a scintillator-PMT detector over a range of ΔE from 300 to 400 eV using a 60 μm objective aperture, a 100 μm spectrometer entrance aperture and an energy resolution of 5 eV.

Results

Calcium oxalate formation in epithelial cells

Calcium oxalate formation in sternal epithelial cells shows a biphasic time course (Fig. 3A). After a lag phase of approximately 15 min, the signal rises first slowly and then

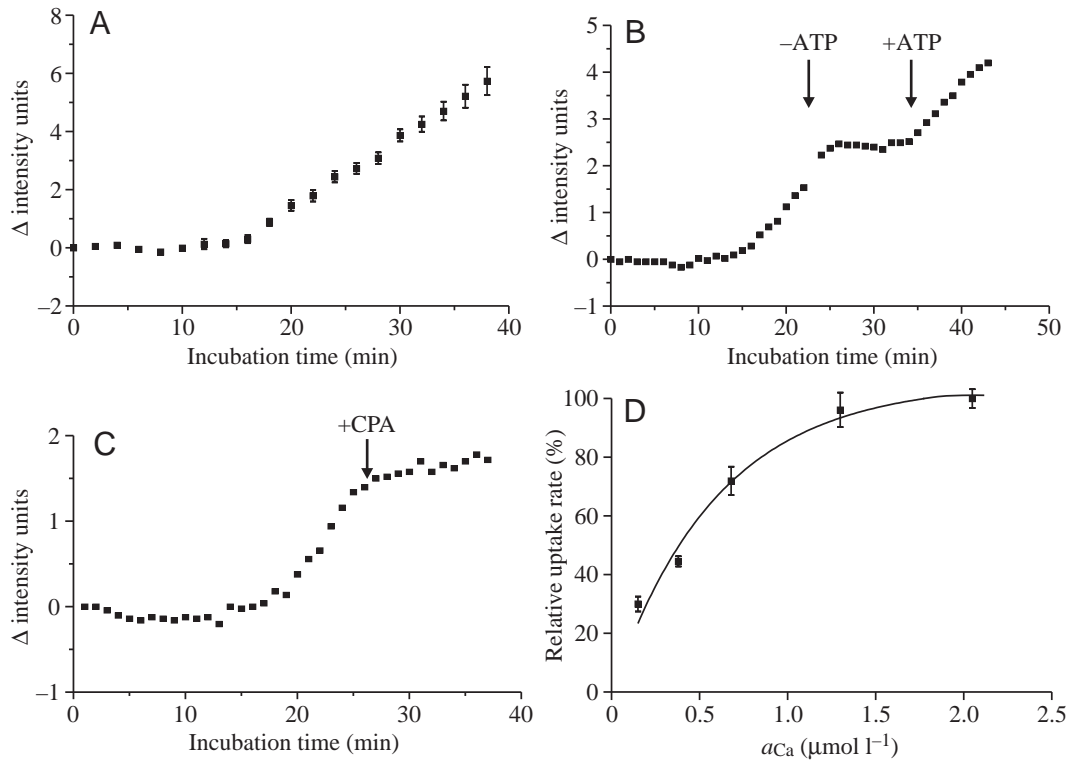


Fig. 3. Calcium oxalate loading experiments in the anterior sternal epithelium of *Porcellio scaber* during late premoult. (A) Intensity signal in the loading medium at a Ca^{2+} activity (a_{Ca}) of $0.68 \mu\text{mol l}^{-1}$. The Δ intensity units given in A–C represent the difference between the mean grey-scale value and that in the first image. Each point represents the mean \pm S.E.M. of nine animals. (B) Effect of ATP on calcium oxalate loading. After removal of Na_2ATP , calcium oxalate loading is immediately and reversibly blocked. (C) Effect of the specific smooth endoplasmic reticulum Ca^{2+} -ATPase inhibitor cyclopiazonic acid (CPA) on calcium oxalate loading at a a_{Ca} of $0.38 \mu\text{mol l}^{-1}$. After addition of $1 \mu\text{mol l}^{-1}$ CPA, the increase in the intensity signal is immediately blocked. (D) Effect of a_{Ca} on calcium oxalate loading in the anterior sternal epithelium from late premoult animals. Each data point gives the mean intensity value (\pm S.E.M.) of 4–6 loading experiments. The rates were normalised to the highest rate at a a_{Ca} of $2.05 \mu\text{mol l}^{-1}$ and plotted against a_{Ca} . The line was drawn using GraphPad Prism 3.0 software.

linearly for up to 1 h. After perfusion with ATP-free loading medium, the increase in optical signal was blocked immediately (Fig. 3B); it resumed after exposure to standard loading medium containing 5 mmol l^{-1} ATP ($N=7$). Exposure to $1 \mu\text{mol l}^{-1}$ CPA, a specific blocker of the SERCA, caused an immediate inhibition of calcium oxalate formation (Fig. 3C). The block by CPA was not affected by changing a_{Ca} to $0.38 \mu\text{mol l}^{-1}$ ($N=2$), $0.68 \mu\text{mol l}^{-1}$ ($N=7$) and $1.3 \mu\text{mol l}^{-1}$ ($N=2$). InsP_3 ($N=7$), ryanodine ($N=5$) and caffeine ($N=4$) had no effect on the rate of calcium oxalate formation. The rate of calcium oxalate formation depended on a_{Ca} within the range 0.15 – $2.05 \mu\text{mol l}^{-1}$ (Fig. 3D), which shows the relative Ca^{2+} uptake rate to have a half-maximum at $0.4 \mu\text{mol l}^{-1}$, indicating that active Ca^{2+} uptake into the SER was stimulated at physiological Ca^{2+} concentrations. The Hill coefficient was 1.8.

Transmission electron microscopy confirmed that the precipitates were formed in the sternal epithelial cells (Fig. 4). Although the cells were permeabilised and incubated in loading medium for a relatively long time, most specimens showed good structural preservation. The oxalate crystals appeared either as large elongated structures (Fig. 4A) or as small needle-like crystals (Fig. 4B).

Electron-dense, calcium-containing precipitates were confined to the cytoplasm and were surrounded by smooth membranes (Fig. 4C,D). It is possible that the smaller crystals resulted from vesiculation of the membranous structures in some cells as a result of the permeabilisation and calcium oxalate loading procedures. Calcium oxalate appeared only occasionally in mitochondria (Fig. 4A,B). Electron energy-loss spectroscopic images of precipitates produced bright signals when the energy loss was switched from 320 to 360 eV, indicating the presence of calcium (Fig. 5A,B). Electron energy-loss spectroscopy of precipitates confirmed this result because of the large signal at the $\text{Ca}_{\text{L}_{2,3}}$ edge at 346 eV (Fig. 5C).

Comparison of Ca^{2+} uptake rate in different moulting stages

Ca^{2+} uptake rates in sternal epithelial cells changed significantly during the moulting cycle (Fig. 6). Calcium oxalate formation increased from undetectable rates in early premoult to considerable rates in mid premoult. A significant increase in calcium oxalate formation occurred between mid premoult (0.045 ± 0.027 intensity units min^{-1}) and late premoult (0.23 ± 0.016 intensity units min^{-1} , $P < 0.001$) and between mid premoult and intramoult (0.19 ± 0.03 intensity units min^{-1} ,

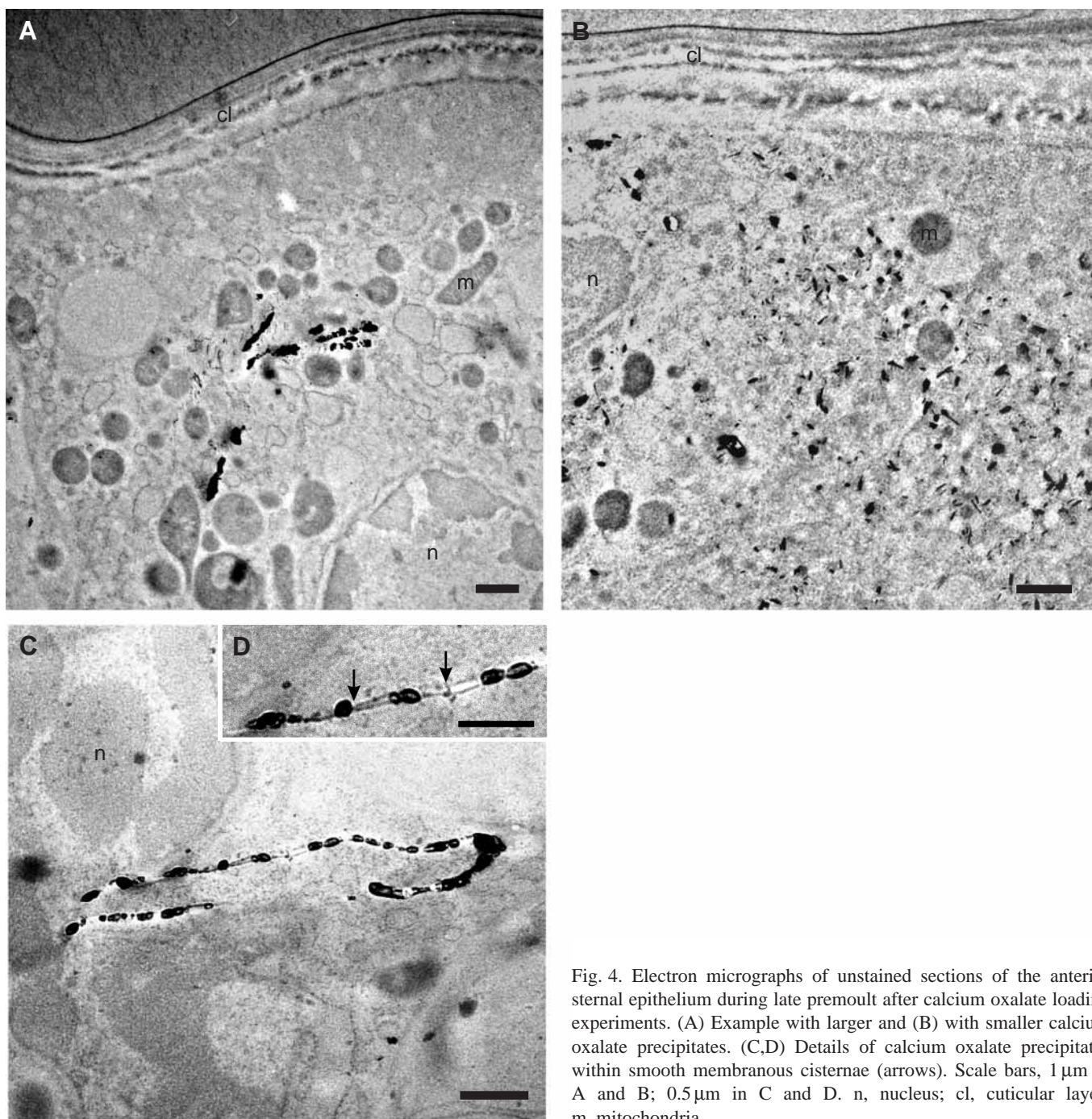


Fig. 4. Electron micrographs of unstained sections of the anterior sternal epithelium during late premoult after calcium oxalate loading experiments. (A) Example with larger and (B) with smaller calcium oxalate precipitates. (C,D) Details of calcium oxalate precipitates within smooth membranous cisternae (arrows). Scale bars, 1 μm in A and B; 0.5 μm in C and D. n, nucleus; cl, cuticular layer; m, mitochondria.

$P < 0.01$) in the anterior sternal epithelium. No significant differences were observed between uptake rates in the anterior and posterior sternal epithelia during the late premoult and intramoult stages. In the posterior sternal epithelium of the early premoult and mid premoult stages, we obtained no conclusive results since we could not separate the cuticle from the epithelium. In these stages, birefringent structures formed within the mineralised cuticle, probably as a result of crystallisation of amorphous CaCO_3 . Generally, a slight and insignificant ($P > 0.05$) decrease in uptake rate was measured between late premoult and intramoult. During intramoult, large

birefringent crystals appeared in the new cuticle of most of the posterior sternal epithelium, again probably as a result of crystallisation of amorphous CaCO_3 within the partly calcified cuticle. These specimens were omitted from the analysis.

Discussion

The calcium oxalate method is a valuable tool for identifying and characterising Ca^{2+} -sequestering organelles *in situ*. It meets all the requirements, such as specificity and linearity, to provide a good approach for monitoring the kinetics of Ca^{2+}

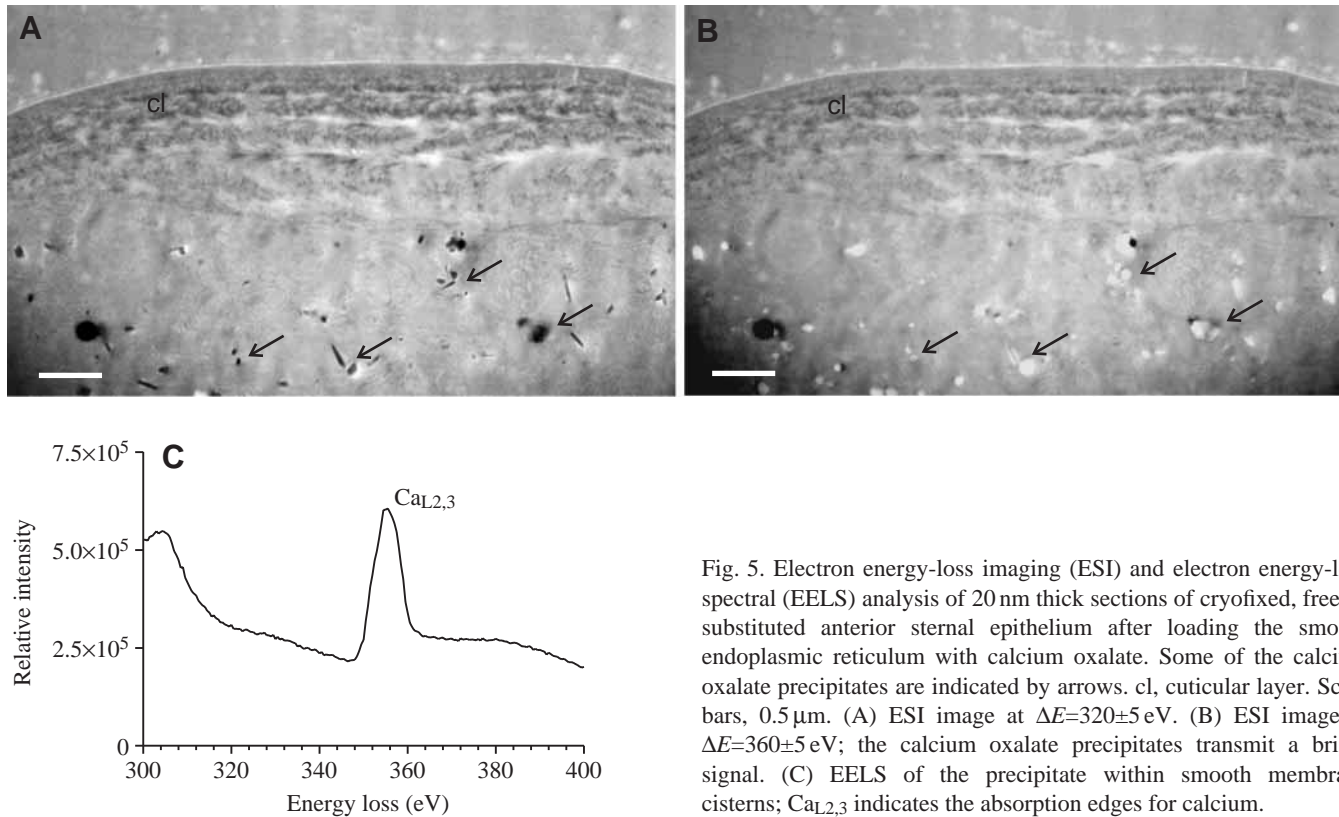


Fig. 5. Electron energy-loss imaging (ESI) and electron energy-loss spectral (EELS) analysis of 20 nm thick sections of cryofixed, freeze-substituted anterior sternal epithelium after loading the smooth endoplasmic reticulum with calcium oxalate. Some of the calcium oxalate precipitates are indicated by arrows. cl, cuticular layer. Scale bars, 0.5 μm . (A) ESI image at $\Delta E=320\pm 5$ eV. (B) ESI image at $\Delta E=360\pm 5$ eV; the calcium oxalate precipitates transmit a bright signal. (C) EELS of the precipitate within smooth membrane cisterns; $\text{Ca}_{L2,3}$ indicates the absorption edges for calcium.

uptake into the SER (Walz, 1982). A comprehensive discussion of this and related methods is given in the review by Walz and Baumann (1989). Here, we use this method to compare SERCA activity in the sternal integument of the terrestrial isopod *Porcellio scaber* among four different moulting stages. For the first time, we report a correlation between the increase in SERCA-dependent Ca^{2+} uptake into the SER and the moult-related increase in epithelial Ca^{2+} transport in Crustacea.

The dependency of calcium oxalate formation on ATP in the sternal epithelial cells of *P. scaber* and its almost total block by cyclopiazonic acid (CPA) indicate a SERCA-mediated sequestration of cytoplasmic Ca^{2+} into membranous compartments. This is supported by the dependency on the Ca^{2+} concentration in the loading medium, with the half-maximal uptake rate at a_{Ca} being $0.4 \mu\text{mol l}^{-1}$. This value is similar to the submicromolar values of calcium oxalate formation found in SER cisternae of photoreceptors in insects (Baumann and Walz, 1989; Walz, 1982) and crayfish (Frixione and Ruiz, 1988). Electron microscopy, electron energy-loss imaging and electron energy-loss spectroscopy verified that the calcium-containing precipitates formed within the epithelial cells of *P. scaber* during a calcium oxalate loading experiment are formed in smooth membranous cisternae, most probably the smooth endoplasmic reticulum.

Within cells, Ca^{2+} functions as a ubiquitous second messenger regulating a vast variety of physiological processes. Ca^{2+} signals are mediated by an influx of extracellular Ca^{2+}

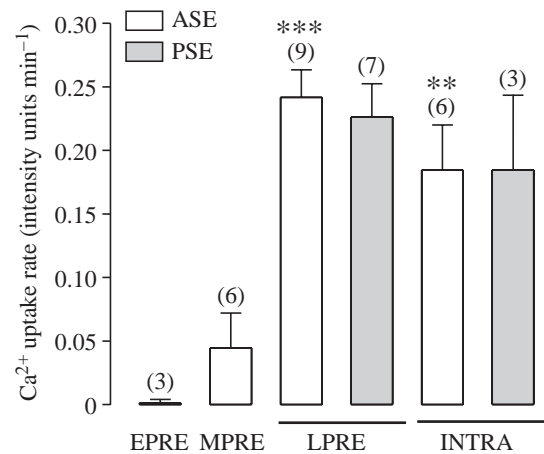


Fig. 6. Comparison of Ca^{2+} uptake rates in sternal epithelial cells at different stages of the moulting cycle (means + s.e.m.). The number of samples is given in parentheses. Asterisks indicate significant differences from the mid premoult stage; *** $P<0.001$, ** $P<0.01$. ASE, anterior sternal epithelium; PSE, posterior sternal epithelium; EPRE, early premoult; MPRE, mid premoult; LPRE, late premoult; INTRA, intramoult.

across Ca^{2+} channels and/or by release of Ca^{2+} from the SER (Berridge, 1993). The SERCA replenishes Ca^{2+} stores by re-uptake of Ca^{2+} into the SER and restores low cytosolic free Ca^{2+} concentrations. In Ca^{2+} -transporting epithelia, in which cytoplasmic Ca^{2+} loads are high, regulation of cytosolic Ca^{2+}

concentrations by the SERCA may be of particular importance. Recently, Simkiss (1996) reviewed the conflict between bulk cytosolic transport of Ca^{2+} in epithelial Ca^{2+} transport, its function as a second messenger and the toxicity of sustained high Ca^{2+} concentrations. Simple diffusion of free Ca^{2+} through the cytosol is impeded by its relatively slow diffusion rate, and increasing the Ca^{2+} gradient from one side of the epithelial cell to the other would result in high and toxic Ca^{2+} concentrations. Therefore, mechanisms including facilitated diffusion by Ca^{2+} -binding proteins (Feher et al., 1989) and compartmentalisation (Simkiss, 1996) have been proposed for transcellular Ca^{2+} transit.

A recent electron-probe X-ray-microanalysis (EPMA) of freeze-dried cryosections of the sternal integument of shock-frozen *P. scaber* revealed high concentrations of *in situ* total (bound plus free) calcium, $[\text{Ca}]_t$, of between 4.5 and 5.7 mmol kg⁻¹ dry mass, suggesting the presence of high concentrations of Ca^{2+} -binding proteins (Ziegler, 2002). However, comparison of $[\text{Ca}]_t$ in the sternal epithelium of *P. scaber* between the early premoult, late premoult and intramoult stages indicates that the concentration of Ca^{2+} -binding proteins does not change throughout the moulting cycle, arguing against a direct role of cytosolic Ca^{2+} -binding proteins in epithelial Ca^{2+} transit. In contrast, the EPMA study demonstrated an *in situ* increase in the number of areas with high $[\text{Ca}]_t$ (15–50 mmol l⁻¹ kg⁻¹ dry mass) between early premoult and intramoult resulting from the contribution of Ca^{2+} 'hot spots' to the analysed area (Ziegler, 2002). The highest values of approximately 50 mmol kg⁻¹ dry mass are similar to those measured in the SER of vertebrate (Jorgensen et al., 1988; Somlyo and Walz, 1985) and invertebrate (Baumann et al., 1991) cells. Comparison of the rates of calcium oxalate formation reported here indicates that the SERCA activity increases from undetectable values in the non- Ca^{2+} -transporting early premoult stage to measurable values in the mid premoult stage, and increases further by a factor of up to five between mid premoult and the Ca^{2+} -transporting late premoult and intramoult stages. This suggests that, in the ASE and the PSE of *P. scaber*, the SER plays a direct role in epithelial Ca^{2+} transit and supports the proposal that the Ca^{2+} 'hot spots' revealed by EPMA represent SER cisternae. A role for the SER in epithelial Ca^{2+} transit was recently suggested in rat dental ameloblasts, in which SERCA activity and SER Ca^{2+} -binding proteins are upregulated during the calcification process (Franklin et al., 2001; Hubbard, 1996).

It is of interest that, in rat dental ameloblasts, the cytoplasmic 28 kDa Ca^{2+} -binding protein calbindin is expressed in high concentrations, although the temporal expression pattern is not consistent with a primary role in Ca^{2+} transport (Hubbard, 1996). This situation seems to be similar to that in the sternal epithelium of *P. scaber*, in which EPMA also suggests a high, but invariable, concentration of Ca^{2+} -binding proteins in the cytosol. Ameloblasts, like the sternal epithelium of *P. scaber*, are involved in mineralisation processes that require massive transport of Ca^{2+} in a very short time. Ca^{2+} flux rates through those epithelia are expected to be much higher than in the kidney

and intestine. It seems possible that organellar routes evolved in mineralising tissues since high Ca^{2+} transit rates generally exceed the capacity of a cytosolic route.

Simkiss (1996) suggested that the loading and discharge of membranous compartments would lead to a vectorial translocation of Ca^{2+} . Another possibility would be that Ca^{2+} diffuses through the lumen of the SER, possibly facilitated by low-affinity Ca^{2+} -binding proteins. Alternatively, the SER could function as a Ca^{2+} buffer to prevent the formation of high cytosolic Ca^{2+} concentrations during SER-independent Ca^{2+} transit. It is important to note that a route through the SER would be in conflict with the SER's role in Ca^{2+} signalling. This conflict could be avoided if functions related to Ca^{2+} signalling and epithelial Ca^{2+} transport were regulated *via* different SERCA isoforms, possibly in different SER subcompartments. Recent investigations have revealed at least four different SERCA isoforms in crayfish tissues (Zhang et al., 2000) and two isoforms in whole brine shrimps (Escalante and Sastre, 1993).

At this stage of the investigation, other routes for Ca^{2+} transit, such as vesicular transport or co-secretion of Ca^{2+} , cannot be ruled out for the sternal epithelium of *P. scaber*. In fact, electron microscopy, electron energy-loss spectroscopy and electron-probe X-ray-microanalysis demonstrated secretion of calcium-, phosphorus- and nitrogen-containing granules at the lateral plasma membranes of the ASE during resorption of the sternal CaCO_3 deposits during intramoult (Glötzner and Ziegler, 2000; Ziegler, 1996, 2002), suggesting co-secretion of protein and Ca^{2+} . A contribution of mitochondria to Ca^{2+} storage and/or transport during epithelial Ca^{2+} transit has also been discussed for several crustacean Ca^{2+} -transporting epithelia (Rogers and Wheatly, 1997; Ueno, 1980). However, electron-probe X-ray-microanalysis of ASE cells of *P. scaber* demonstrated a decrease in the total mitochondrial calcium concentration rather than an increase between early premoult and late premoult and between early premoult and intramoult (Ziegler, 2002), excluding the possibility that mitochondria could store or transport Ca^{2+} during Ca^{2+} transit.

As a working hypothesis, we propose that in *Porcellio scaber* the SER actively contributes to Ca^{2+} transit through the ASE and PSE cells during the formation and resorption of the CaCO_3 deposits. Future investigations should attempt to develop methods for the direct monitoring of epithelial Ca^{2+} transport and the use of pharmacological tools to analyse the role of the SER in epithelial Ca^{2+} transport.

We thank Dr Tom Carefoot for critically reading the manuscript and Oliver Schmid for his help in optimising the calcium oxalate assay. This work was supported by the Deutsche Forschungsgemeinschaft Zi 368/3-3.

References

- Ahearn, G. A. and Franco, P. (1990). Sodium and calcium share the electrogenic $2\text{Na}^+-1\text{H}^+$ antiporter in crustacean antennal glands. *Am. J. Physiol.* **259**, F758–F767.
- Ahearn, G. A. and Franco, P. (1993). Ca^{2+} transport pathways in brush-

- border membrane vesicles of crustacean antennal glands. *Am. J. Physiol.* **264**, 1206–1213.
- Ahearn, G. A. and Zhuang, Z.** (1996). Cellular mechanisms of calcium transport in crustaceans. *Physiol. Zool.* **69**, 383–402.
- Baumann, O. and Walz, B.** (1989). Calcium- and inositol polyphosphate-sensitivity of the calcium-sequestering endoplasmic reticulum in the photoreceptor cells of the honeybee drone. *J. Comp. Physiol. A* **165**, 627–636.
- Baumann, O., Walz, B., Somlyo, A. V. and Somlyo, A. P.** (1991). Electron probe microanalysis of calcium release and magnesium uptake by endoplasmic reticulum in bee photoreceptors. *Proc. Natl. Acad. Sci. USA* **88**, 741–744.
- Berridge, M. J.** (1993). Inositol trisphosphate and calcium signalling. *Nature* **361**, 315–325.
- Drobne, D. and Štrus, J.** (1996). Moulting frequency of the isopod *Porcellio scaber*, as a measure of zinc-contaminated food. *Env. Toxicol. Chem.* **15**, 126–130.
- Escalante, R. and Sastre, L.** (1993). Similar alternative splicing events generate two sarcoplasmic or endoplasmic reticulum Ca-ATPase isoforms in the crustacean *Artemia franciscana* and in vertebrates. *J. Biol. Chem.* **268**, 14090–14095.
- Feher, J. J., Fullmer, C. S. and Fritsch, G. K.** (1989). Comparison of the enhanced steady-state diffusion of calcium by calbindin-D9K and calmodulin: possible importance in intestinal calcium absorption. *Cell Calcium* **10**, 189–203.
- Flik, G., Verboost, P. M. and Atsma, W.** (1994). Calcium transport in gill plasma membranes of the crab *Carcinus maenas*: evidence for carriers driven by ATP and a Na⁺ gradient. *J. Exp. Biol.* **195**, 109–122.
- Franklin, I., Winz, R. and Hubbard, M.** (2001). Endoplasmic reticulum Ca-ATPase pump is up-regulated in calcium-transporting dental enamel cells: a non-housekeeping role for SERCA2b. *Biochem. J.* **358**, 217–224.
- Fruxione, E. and Ruiz, L.** (1988). Calcium uptake by smooth endoplasmic reticulum of peeled retinal photoreceptors of the crayfish. *J. Comp. Physiol. A* **162**, 91–100.
- Glötzner, J. and Ziegler, A.** (2000). Morphometric analysis of the plasma membranes in the calcium transporting sternal epithelium of the terrestrial isopods *Ligia oceanica*, *Ligidium hypnorum* and *Porcellio scaber*. *Arthropod Struct. Dev.* **29**, 241–257.
- Greenaway, P.** (1985). Calcium balance and moulting in the Crustacea. *Biol. Rev.* **60**, 425–454.
- Greenaway, P., Dillaman, R. M. and Roer, R. D.** (1995). Quercetin-dependent ATPase activity in the hypodermal tissue of *Callinectes sapidus*, during the moulting cycle. *Comp. Biochem. Physiol.* **111A**, 303–312.
- Hubbard, M. J.** (1996). Abundant calcium homeostasis machinery in rat dental enamel cells. Up-regulation of calcium store proteins during enamel mineralization implicates the endoplasmic reticulum in calcium transcytosis. *Eur. J. Biochem.* **239**, 611–623.
- Jorgensen, A. O., Broderick, R., Somlyo, A. P. and Somlyo, A. V.** (1988). Two structurally distinct calcium storage sites in rat cardiac sarcoplasmic reticulum: an electron microprobe analysis study. *Circ. Res.* **63**, 1060–1069.
- Messner, B.** (1965). Ein morphologisch-histologischer Beitrag zur Häutung von *Porcellio scaber* Latr. und *Oniscus asellus* I. (Isopoda Terrestria). *Crustaceana* **9**, 285–301.
- Nemere, I.** (1992). Vesicular calcium transport in chick intestine. *J. Nutr.* **122**, 657–661.
- Neufeld, D. S. and Cameron, J. N.** (1993). Transepithelial movement of calcium in crustaceans. *J. Exp. Biol.* **184**, 1–16.
- Roer, R. D.** (1980). Mechanisms of resorption and deposition of calcium in the carapace of the crab *Carcinus maenas*. *J. Exp. Biol.* **88**, 205–218.
- Rogers, J. V. and Wheatly, M. G.** (1997). Accumulation of calcium in the antennal gland during the molting cycle of the freshwater crayfish *Procambarus clarkii*. *Invert. Biol.* **116**, 248–254.
- Simkiss, K.** (1996). Calcium transport across calcium-regulated cells. *Physiol. Zool.* **69**, 343–350.
- Somlyo, A. P. and Walz, B.** (1985). Elemental distribution in *Rana pipiens* retinal rods: quantitative electron probe analysis. *J. Physiol., Lond.* **358**, 183–195.
- Somlyo, A. V., Gonzalez-Serratos, H., Shuman, H., McClellan, G. and Somlyo, A. P.** (1981). Calcium release and ionic changes in the sarcoplasmic reticulum of tetanized muscle: an electron-probe study. *J. Cell Biol.* **90**, 577–594.
- Steel, C. G. H.** (1993). Storage and translocation of integumentary calcium during the moulting cycle of the terrestrial isopod *Oniscus asellus* (L.). *Can. J. Zool.* **71**, 4–10.
- Tsien, R. Y. and Rink, T. J.** (1980). Neutral carrier ion-selective microelectrodes for measurement of intracellular free calcium. *Biochim. Biophys. Acta* **599**, 623–638.
- Ueno, M.** (1980). Calcium transport in crayfish gastrolith disc: morphology of gastrolith disc and ultrahistochemical demonstration of calcium. *J. Exp. Zool.* **213**, 161–171.
- Walz, B.** (1982). Ca²⁺-sequestering smooth endoplasmic reticulum in an invertebrate photoreceptor. II. Its properties as revealed by microphotometric measurements. *J. Cell Biol.* **93**, 849–859.
- Walz, B. and Baumann, O.** (1989). Calcium-sequestering cell organelles: *in situ* localization, morphological and functional characterization. *Progr. Histochem. Cytochem.* **20**, 1–47.
- Wheatly, M. G.** (1997). Crustacean models for studying calcium transport: the journey from whole organisms to molecular mechanisms. *J. Mar. Biol.* **77**, 107–125.
- Zhang, Z., Chen, D. and Wheatly, M. G.** (2000). Cloning and characterization of sarco/endoplasmic reticulum Ca²⁺-ATPase (SERCA) from crayfish axial muscle. *J. Exp. Biol.* **203**, 1–13.
- Ziegler, A.** (1994). Ultrastructure and electron spectroscopic diffraction analysis of the sternal calcium deposits of *Porcellio scaber* Latr. (Isopoda, Crustacea). *J. Struct. Biol.* **112**, 110–116.
- Ziegler, A.** (1996). Ultrastructural evidence for transepithelial calcium transport in the anterior sternal epithelium of the terrestrial isopod *Porcellio scaber* (Crustacea) during the formation and resorption of CaCO₃ deposits. *Cell Tissue Res.* **284**, 459–466.
- Ziegler, A.** (1997). Immunocytochemical localization of Na⁺,K⁺-ATPase in the calcium-transporting sternal epithelium of the terrestrial isopod *Porcellio scaber* Latr. (Crustacea). *J. Histochem. Cytochem.* **45**, 437–446.
- Ziegler, A.** (2002). X-ray microprobe analysis of epithelial calcium transport. *Cell Calcium* (in press).
- Ziegler, A. and Scholz, F. H. E.** (1997). The ionic hemolymph composition of the terrestrial isopod *Porcellio scaber* Latr. during molt. *J. Comp. Physiol. B* **167**, 536–542.
- Ziegler, A., Weihrauch, D. and Towle, D. W.** (2001). Increased expression of the Ca²⁺-ATPase and the Na⁺/Ca²⁺-exchanger in the anterior sternal tissue of *Porcellio scaber* (Isopoda, Crustacea) during premolt. *Zoology* **104**, Suppl. IV, 67.